

Minimum and Complete Fluidization Velocity for Sand-Palm Shell Mixtures, Part II: Characteristic Velocity Profiles, Critical Loading and Binary Correlations

¹V.S. Chok, ²A. Gorin and ²H.B. Chua

¹Department of Chemical Engineering, University Technology PETRONAS,
31750 Tronoh, Perak, Malaysia

²School of Engineering and Science, Department of Chemical Engineering,
Curtin University of Technology Sarawak Campus,
CDT 250, 98009 Miri, Sarawak, Malaysia

Abstract: Problem statement: In Part I of this research, the main features of the fluidization behavior and characteristic velocities had been reported. **Approach:** In the present research, the mixtures characteristic velocity profiles for various sand sizes, palm shell sizes and weight percents were presented. It was recognized that there are instances where the characteristic values remain nearly unchanged from its pure sand values. This regime of constant values can be observed in both compartments and can be established depending on the bed properties. The term “Critical loading” is then selected to define the maximum palm shell content (size and weight percent) that can be present in the mixtures where the characteristic velocities remain absolutely of pure sand values. **Results:** The critical loading increases with the increase of sand size but decreases with the increase of palm shell size. Moreover, it can be observed that the critical loading generally decreases with the increase in particle size ratio, although exception is sighted in the combustor for the mixture with the largest sand size. Overall, the largest sand size has the highest critical loading. Meanwhile, the selected correlations are able to describe the qualitative variation in the characteristic velocities. However, quantitatively, these correlations are unsatisfactory as they are either over-estimate or under-estimate. **Conclusion/Recommendations:** It is desirable to establish the regime of critical loading since the mixture characteristic velocities can be pre-determined using bed material properties made up from pure sand (inert) values. Within this regime, a single operational velocity can be set for respective compartment that is independent from variation of palm shell size and weight percent in the mixtures (especially during combustion or gasification). Ultimately, the state of fluidization (e.g., bubbling or vigorously fluidized) and mixing/segregation condition that depend on relative magnitude of operational and characteristic velocities can be identified and maintained.

Key words: Biomass mixing, fluidization velocity, binary correlations

INTRODUCTION

Palm shell cannot be fluidized solely. It is considered as Geldart D particle, a classification for spouting material. However, the addition of a second fluidizable material (sand) in palm shell can facilitate proper fluidization. In Part I of this research (Chok *et al.*, 2009a), the main features of the fluidization behaviour and characteristic velocities using sand-palm shell mixtures were examined with respect to different bed properties. Their distinct patterns and further analysis on the various characteristic velocity relationships

provide insights on the fluidization mechanism and the mixing/segregation tendency. Some interesting works are given in (Chok *et al.*, 2009b; 2007; Fauziah *et al.*, 2008) on hydrodynamic studies of sand-palm shell mixtures. Interested readers are encouraged to refer to them.

The present study reports the characteristic velocity profiles for various sand sizes, palm shell sizes and weight percent in the mixtures and in different compartments. As described later, it is recognized that there are some instances where the mixtures U_{mf} and U_{cf} values remain nearly unchanged from its pure sand values.

Corresponding Author: V.S. Chok, Department of Chemical Engineering, University Technology PETRONAS, 31750 Tronoh, Perak, Malaysia

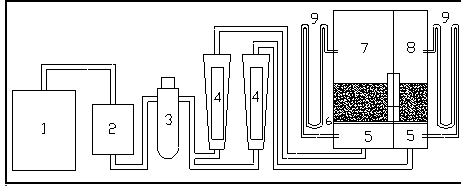


Fig. 1: Experimental setup (1) compressor; (2) dryer; (3) pressure regulator; (4) rotameter; 5: plenum; (6) perforated distributor; (7) combustor; (8) gasifier; (9) manometer (Chok *et al.*, 2009a)

This regime of constant U_{mf} and U_{cf} values can be observed in both compartments and can be established depending on the bed properties.

It is desirable to establish this regime for each compartment since the mixture characteristic velocities can be pre-determined using the bed material properties made up from entirely pure sand (inert) values. Within this regime, a single operational velocity can be set for the respective compartment based on the pure sand value and is independent from the variation of the palm shell size and weight percent in the mixtures (especially during combustion or gasification). Ultimately, the state of fluidization (e.g., bubbling or vigorously fluidized) and the condition of mixing/segregation in each compartment, that depend on the relative magnitude of the operational and characteristic velocities can be identified and maintained. Therefore, it is of great advantage to determine this regime for each compartment and the term “critical loading” is selected.

Meanwhile, various published U_{mf} and U_{cf} correlations are tested and compared with the experimental values.

MATERIALS AND METHODS

As the apparatus for this study is the same as described in (Chok *et al.*, 2009a), only a brief description is included here. A schematic of the experimental setup is illustrated in Fig. 1. The cold flow model as shown in Fig. 2 has a 0.66 ID and is divided into 2 compartments i.e. combustor and gasifier by a vertical wall in 2:1 cross-sectional area ratio. The effective diameters, D_e are computed as 25.7 and 41.3 cm for gasifier and combustor respectively (Chok *et al.*, 2009a).

The experiments were carried out in both of the compartments at 0.4 m static bed height. Large amount of bed material is used, i.e., 77 and 101 kg respectively. 4 different types of sand and palm shell sizes are selected as the bed materials. The physical properties of the sand and palm shell are given in Table 1.

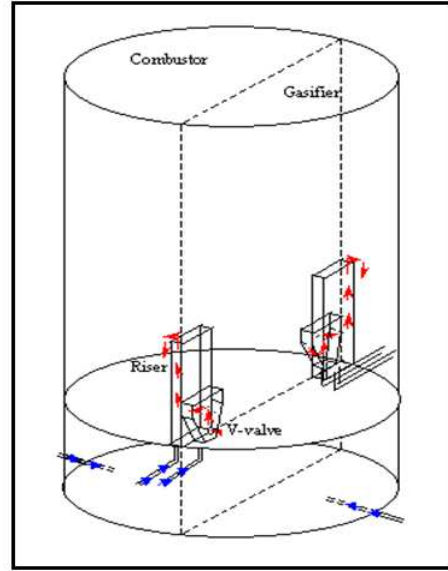


Fig. 2: Isometric view of CFBG (Chok *et al.*, 2009a)

Table 1: Palm shell and sand properties

| Properties | Palm shell | Sand |
|---------------------------------|---------------------|-------|
| Particle size/sieved range (mm) | 1.77/(+1.18-2.36) | 0.196 |
| | 3.56/(+2.36-4.75) | 0.272 |
| | 7.13/(+4.75-9.50) | 0.341 |
| | 11.75/(+9.50-14.00) | 0.395 |
| Density (kg m ⁻³) | 1,500 | 2,700 |
| Moisture (wt%) | 8-10% | - |
| Weight percent (wt%) | 2, 5, 10 and 15% | - |

RESULTS

Characteristic velocity profiles: Figure 3 shows the U_{mf} and U_{cf} profiles in the combustor at various palm shell sizes and weight percent with finest sand of 196 μm . For the smallest size palm shell of +1.18-2.36 mm, both the U_{mf} and U_{cf} values remain unchanged from the values of pure sand as in (Chok *et al.*, 2009a). Similarly, for medium size palm shell of +2.36-4.75 mm, these values remain constant except at 15 wt%. With larger palm shell size of +4.75-9.50 mm, the characteristic value changes at 5-10 wt% but further increase of palm shell leads to severe channeling. This channeling condition is also observed for the largest palm shell size of +9.50-14.00 mm where the characteristic velocities increase with the increase of palm shell wt% only up to 5wt%. Settlement of palm shell “chunks” are observed at higher weight percent for palm shell of >4.75 mm even at the maximum capacity of air flow rate (10 times U_{mf} of pure sand). Consequently, data that are not shown are due to poor fluidization.

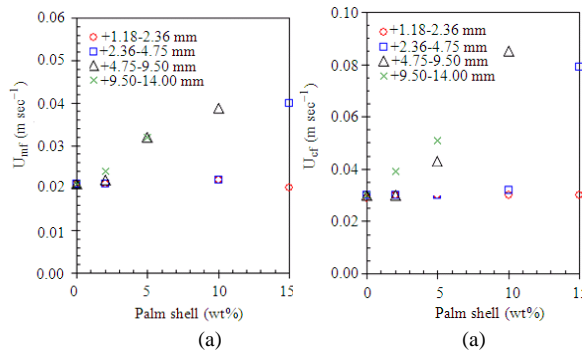


Fig. 3a and b: U_{mf} and U_{cf} in the combustor; sand of $196 \mu\text{m}$ and palm shell of various sizes and weight percent

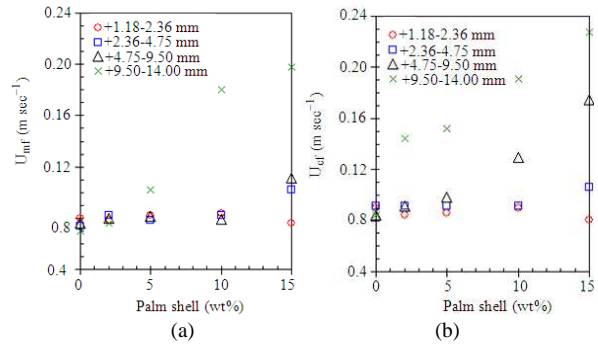


Fig. 5a and b: U_{mf} and U_{cf} in the gasifier; sand of $272 \mu\text{m}$ and palm shell of various sizes and weight percent

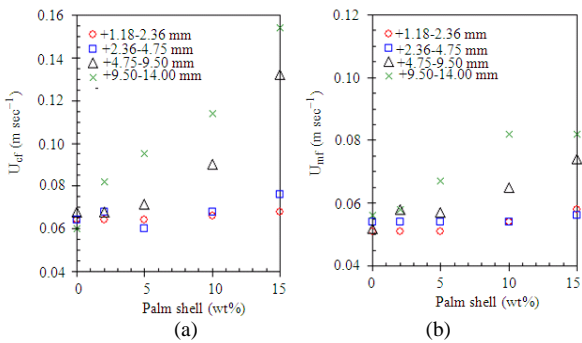


Fig. 4a and b: U_{mf} and U_{cf} in the combustor; sand of $272 \mu\text{m}$ and palm shell of various sizes and weight percent

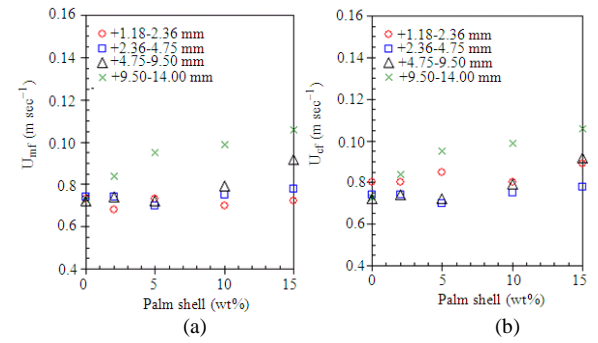


Fig. 6a and b: U_{mf} and U_{cf} in the combustor; sand of $341 \mu\text{m}$ and palm shell of various sizes and weight percent

Figure 4a and 5a indicate the U_{mf} values for gasifier and combustor at various palm shell sizes and wt% with river sand of $273 \mu\text{m}$.

The U_{mf} values remain unchanged in the combustor for palm shell size $<4.75 \text{ mm}$. Although similarly is found in the gasifier, the U_{mf} increases at palm shell of $+2.36-4.75 \text{ mm}$ at 15 wt\% . The U_{mf} increases at ≥ 10 and $\geq 5 \text{ wt\%}$ for palm shell of $+4.75-9.50$ and $+9.50-14.00 \text{ mm}$ respectively in the combustor. However, in the gasifier, the effect of palm shell of $+4.75-9.50$ and $+9.50-14.00 \text{ mm}$ to the U_{mf} is noticeable at 15 wt\% and $\geq 5 \text{ wt\%}$ respectively.

The Fig. 4b and 5b indicate the U_{cf} values for gasifier and combustor using the same river sand and palm shell composition. For palm shell size $<4.75 \text{ mm}$, the U_{cf} values in both compartments remain nearly unchanged except palm shell of $+2.36-4.75 \text{ mm}$ at 15 wt\% in the gasifier. For palm shell size of $+4.75-9.50 \text{ mm}$, U_{cf} values for gasifier and combustor begin to show upward trends at $\geq 10 \text{ wt\%}$.

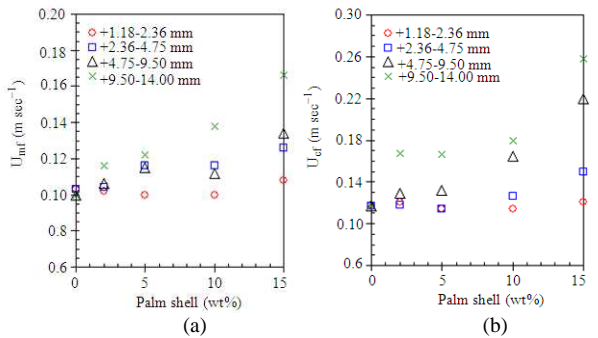


Fig. 7a and b: U_{mf} and U_{cf} in the gasifier; sand of $341 \mu\text{m}$ and palm shell of various sizes and weight percent

Figure 6a and 7a indicate the U_{mf} values for combustor and gasifier at various palm shell sizes and wt% with larger sand of $341 \mu\text{m}$. No changes in the U_{mf} for palm shell size $<9.50 \text{ mm}$ in the combustor, except for palm shell of $+4.75-9.50 \text{ mm}$ at 15 wt\% . This trend

is also similarly observed in the gasifier, but with significant U_{mf} increase for palm shell of 2.36-4.75 and +4.75-9.50 mm at 15 wt%. In addition, for palm shell >9.50 mm, at ≥ 2 wt%, increase of U_{mf} was observed in both compartments.

Figure 6b and 7b above indicate the U_{cf} values for combustor and gasifier at various palm shell sizes and wt% with quartz sand of 341 μm . No changes in the U_{cf} for palm shell size <4.75 mm in the combustor. Similar trend is also obtained in the gasifier except a noticeable U_{cf} increase for palm shell of +2.36-4.75 mm at 15 wt%. For palm shell of +4.75-9.50 mm in the combustor, there is a marginal U_{cf} increase at 15 wt%. A steep increase in U_{cf} is observed in the gasifier for palm shell of +4.75-9.50 mm at ≥ 10 wt%. For palm shell of +9.50-14.00 mm, incremental in U_{cf} values are observed at ≥ 2 wt%.

Figure 8 and 9 indicate the U_{mf} and U_{cf} values for combustor and gasifier at various palm shell sizes and wt% with quartz sand of 395 μm .

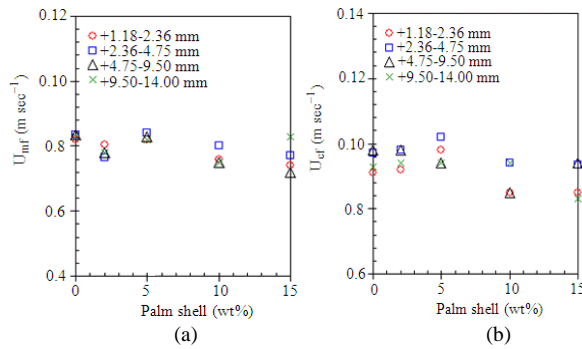


Fig. 8a and b: U_{mf} and U_{cf} in the combustor; sand of 395 μm and palm shell of various sizes and weight percent

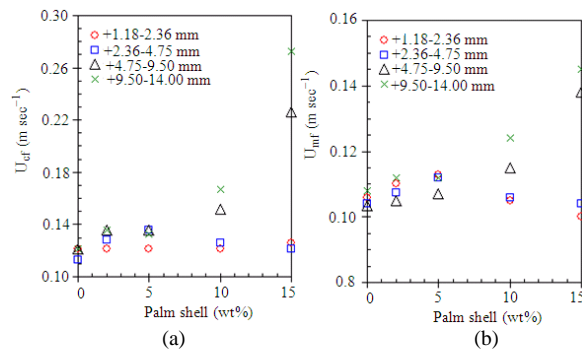


Fig. 9a and b: U_{mf} and U_{cf} in the gasifier; sand of 395 μm and palm shell of various sizes and weight percent

As shown in Fig. 8a, the U_{mf} values in the combustor are relatively constant for all palm shell sizes at ≤ 5 wt%. However, slight decrease in the U_{mf} values are observed for palm shell sizes of ≤ 9.50 mm at ≥ 10 wt%. For the largest palm shell size of +9.50-14.00 mm, the U_{mf} values remain unchanged. Similarly, in Fig. 8b, the U_{cf} values in the combustor remain nearly unchanged for all palm shell sizes at ≤ 5 wt%. However, slight decrease in the U_{cf} values at 10 wt% is noticeable for palm shell of +1.18-2.36 mm and +4.75-9.50 mm. For the largest palm shell size of +9.50-14.00 mm, the U_{cf} values remain unchanged up to 10 wt% and decreases at 15 wt%.

In Fig. 9a, the U_{mf} values for palm shell of ≤ 4.75 mm remains fairly constant up to 15 wt% in the gasifier. However, for palm shell size of ≥ 4.75 mm, at ≥ 10 wt%, increase of U_{mf} values are observed. Similarly found in Fig. 9b, the U_{cf} values for palm shell of ≤ 4.75 mm remains constant in the gasifier. For palm shell size ≥ 4.75 mm, at ≥ 10 wt%, increase of U_{cf} values are observed.

Critical loading: Based on all the characteristic velocity profiles shown in Fig. 3-9, it is recognized that there are some instances where the mixtures U_{mf} and U_{cf} values remain nearly unchanged from its pure sand values. Therefore, it is of great advantage to determine this regime for each compartment and the term “critical loading” is selected. “Critical loading” is defined here as the maximum palm shell content (size and weight percent) that can be present in the sand where the mixtures U_{mf} and U_{cf} values remain absolutely of pure sand values. These values (of pure sand and mixture) are considered identical when the respective characteristic velocities variations between the bed materials are within $\pm 15\%$. Table 2 and 3 show the critical loading for U_{mf} and U_{cf} in the combustor and gasifier respectively.

Table 2: Critical loading for u_{mf} and u_{cf} in the combustor

| Sand size (μm) | Palm shell size (mm) | | | |
|-----------------------------|----------------------|------------|------------|-------------|
| | +1.18-2.36 | +2.36-4.75 | +4.75-9.50 | +9.50-14.00 |
| 196 | 15/(15) | 10/(5) | 2/(2) | 2/(0) |
| 272 | 15/(15) | 15/(10) | 5/(5) | 2/(0) |
| 341 | 15/(15) | 15/(10) | 10/(5) | 2/(2) |
| 395 | 15/(15) | 15/(15) | 15/(15) | 15/(10) |

Table 3: Critical loading for u_{mf} and u_{cf} in the gasifier

| Sand size (μm) | Palm shell size (mm) | | | |
|-----------------------------|----------------------|------------|------------|-------------|
| | +1.18-2.36 | +2.36-4.75 | +4.75-9.50 | +9.50-14.00 |
| 196 | - | - | - | - |
| 272 | 15/(15) | 10/(10) | 10/(5) | 2/(0) |
| 341 | 15/(15) | 10/(10) | 10/(5) | 2/(0) |
| 395 | 15/(15) | 15/(15) | 10/(10) | 5/(5) |

In both Table 2 and 3, it can be seen that for the smallest palm shell size of +1.18-2.36 mm, up to 15 wt% can be present in the mixture with any sand sizes without resulting significant changes in the mixture characteristic velocities from the pure sand values.

In addition, the critical loading increases with the increase of sand size but decreases with the increase of palm shell size. Meanwhile, the critical loading for the U_{mf} is always equal or larger than the U_{cf} value in both of the compartments. Overall, the largest sand size (395 μ m) has the highest critical loadings in both of the characteristic velocities.

Fig. 10 and 11 show the critical loading as a function of particle size ratio (palm shell/sand) in the combustor and gasifier respectively. The area below the lines and bounded by the horizontal axis represent the regime of the critical loading at various mixture size and composition. Generally, it can be observed that the critical loading decreases with the increase in particle size ratio i.e., in the trend of reducing. However, the formations of intermediate peaks occur in the combustor as shown in Fig. 10 for the mixture with sand of 395 μ m. This is due to the increased in particles mixing as described earlier (Refer to Ratio of U_{cf}/U_{mf}) as observed in the larger compartment. In addition, the critical loading line for the U_{mf} always lie on or above the values for the U_{cf} .

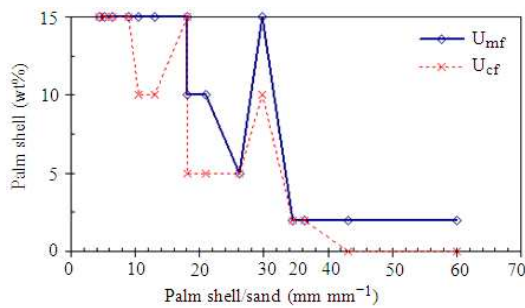


Fig. 10: Critical loading in the combustor

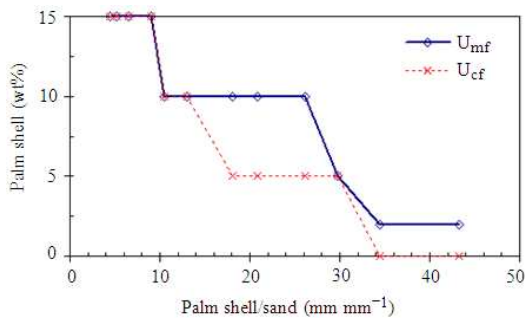


Fig. 11: Critical loading in the gasifier

U_{mf} and U_{cf} values comparison with correlations:

The U_{mf} and U_{cf} values for sand/palm shell mixtures determined using the common methods for multi-components system allow comparative studies to be carried out from the various published correlations.

Three different binary correlations namely Mourad *et al.* (1994); Goosens *et al.* (1971) and Thonglimp *et al.* (1984) are selected for comparison with experimental U_{mf} values. In addition, 4 different binary correlations namely Noda *et al.* (1986); Gauthier *et al.* (1999) and Rao *et al.* (2001) are selected for comparison with experimental U_{cf} values. These researchers also utilized similar bed material properties and/or Geldart classification. The characteristic values for mixtures within the critical loading are not included since the mixtures U_{mf} and U_{cf} remain unchanged from the pure sand values.

In Fig. 12, it can be seen that all the U_{mf} correlations generally are able to describe the qualitative variation in the sand-palm shell binary mixtures, i.e., the correlations are able to show the increasing or decreasing trends with respect to different sand-palm shell composition. However, as shown in Fig. 13, quantitatively, most correlations are unsatisfactory as they are either over-estimate or under-estimate these values.

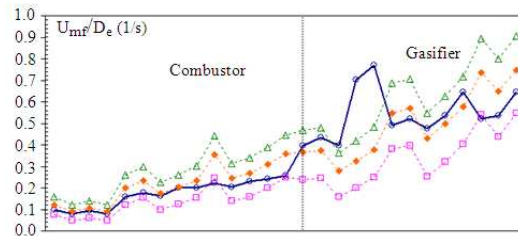


Fig. 12: Comparison of experimental (EXP) U_{mf} / D_e with correlations; (○) (EXP); (□) Mourad *et al.* (1994); (◇) Goosens *et al.* (1971); (△) Thonglimp *et al.* (1984)

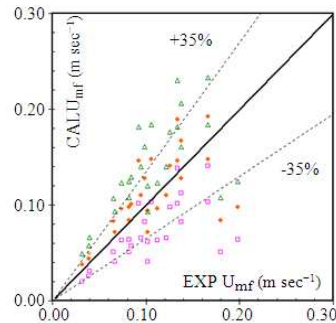


Fig. 13: Comparison of experimental (EXP) U_{mf} with correlations; (□) Mourad *et al.* (1994); (◇) Goosens *et al.* (1971); (△) Thonglimp *et al.* (1984)

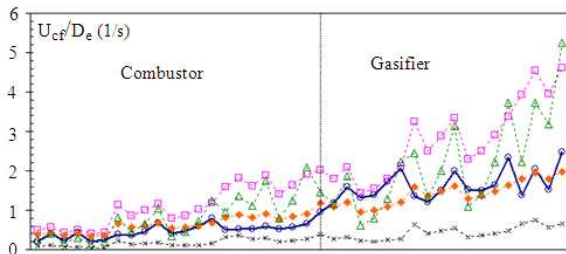


Fig. 14: Comparison of experimental (EXP) U_{cf}/D_e with correlations; (●) (EXP); (□) Mourad *et al.* (1994); (×) Noda *et al.* (1986); (◆) Gauthier *et al.* (1999); (△) Rao *et al.* (2001)

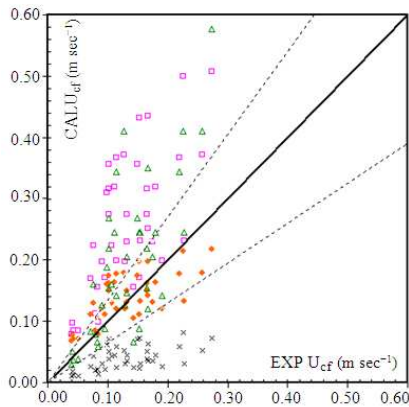


Fig. 15: Comparison of experimental (EXP) U_{cf} with correlations; (□) Mourad *et al.* (1994); (×) Noda *et al.* (1986); (◆) Gauthier *et al.* (1999); (△) Rao *et al.* (2001)

Similar found in Fig. 14 and 15, all the U_{cf} correlations generally shows the qualitative U_{cf} variation for the sand-palm shell binary mixtures but unable to give satisfactory prediction. The results from the various comparisons made on the existing U_{mf} and U_{cf} correlations at different palm shell and sand mixtures clearly show that significant deviation exceeding $\pm 35\%$ from experimental values.

DISCUSSION

On one hand, using smaller sand particle reduces the superficial velocity necessary to establish fluidization when the palm shell components are smaller in sizes or weight percent in the mixtures. However, the tendency for segregation to occur is higher when the resulting particle size ratio (palm shell/sand) is higher due to the lower contribution of particle-particle collision (Chok *et al.*, 2009b).

Consequently, higher superficial velocities are necessary to fluidize the bed mixtures especially if there is any formation of palm shell “chunks” that is enhanced by the present of larger palm shell size and weight percent.

To the contrary, when utilizing large sand particle in the mixture, although greater superficial velocity is required as compared to smaller sand size in order to establish fluidization when palm shell is smaller in sizes or weight percent, the tendency for segregation to occur reduces when the resulting particle size ratio is lower due to the greater contribution of particle-particle collision (Chok *et al.*, 2009b). In addition, the critical loading increases allowing greater proportion of palm shell in all sizes to be present in the mixture without any significant increase of the mixture characteristic velocities from the pure sand value. This condition can be established in both compartments.

CONCLUSION

Taking into account all of the U_{mf} and U_{cf} values at different palm shell and sand mixtures and fitting all these curves to a single mathematical equation is seemingly impractical. Although for a specific palm shell size and sand, U_{mf} and U_{cf} can be fitted into an equation but no correct equation and model which can correlate all of the data that have been found thus far. Direct utilizing of the experimental values for the operation of sand-palm shell in fluidized bed is essential. Alternatively, identifying the critical loading for this mixture provides a convenient yet robust system where its operational velocity can be pre-determined using bed material properties made up from entirely pure sand (inert) values.

REFERENCES

Chok, V.S., S.K. Wee, A. Gorin and H.B. Chua, 2009a. Effect of particle and bed diameter on characteristic velocities in Compartmented Fluidized Bed Gasifier. Proceeding of the 2nd CUTSE International Conference: Progress in Science and Engineering for Sustainable Development, Nov. 24-25, Curtin University of Technology, Sarawak, Malaysia, pp: 1-5.

Chok, V.S., A. Gorin and H.B. Chua, 2009b. Minimum and complete fluidization velocity for sand/palm shell binary mixtures, Part I: Fluidization behavior and characteristic velocities. Proceeding of the 2nd CUTSE International Conference: Progress in Science and Engineering for Sustainable Development, Nov. 24-25, Curtin University of Technology, Sarawak, Malaysia, pp: 1-5.

- Chok, V.S., L.F.B. Chin, S.K. Wee, W.W. Tang and A. Gorin, 2007. Hydrodynamics studies of sand/palm shells binary mixtures in Compartmented Fluidized Bed Gasifier (CFBG). Proceeding of the 1st Engineering Conference on Energy and Environment, Dec. 2007, UNIMAS, Kuching, Sarawak, pp: 301-306.
- Fauziah, M., A.R. Nornizar, A. Nornizar, A. Azil Bahari and M.J. Tajuddin, 2008. Cold flow binary fluidization of oil palm residues mixture in a gas-solid fluidized bed system. *Pertanika J. Sci. Technol.*, 16: 201-212.
- Gauthier, D., S. Zerguerras and G. Flamant, 1999. Influence of the particle size distribution of powders on the velocities of minimum and complete fluidization. *Chem. Eng. J.*, 74: 181-196, DOI: 10.1016/S1385-8947(99)00075-3
- Goosens, W.A.R., G.L. Dumont and G.J. Spaepen, 1971. Fluidization of binary mixtures in the laminar flow reaction. *AIChE Symp. Ser.*, 67: 38-45.
- Mourad, M., M. Hemati and C. Laguerie, 1994. Hydrodynamics of fluidized bed dryer: Determination of characteristics of fluidization velocities of mixtures of corn and sand, *Powder Technol.*, 80: 45-54, DOI: 10.1016/0032-5910(94)87004-7
- Noda, K., S. Uchida, T. Makino and H. Kamo, 1986. Minimum fluidization velocity of binary mixtures of particles with large size ratio. *Powder Technol.*, 46: 149-154. DOI: 10.1016/0032-5910(86)80021-3
- Rao, R., T. Ram and J.V. Bheemarasetti, 2001. Minimum fluidization velocity of mixtures of biomass and sands. *Energy*, 26: 633-644. DOI: 10.1016/S0360-5442(01)00014-7
- Thonglimp, V., N. Hiquily and C. Laguerie, 1984. Minimum fluidization velocity and expansion of layers of mixtures of particulates solids fluidized by a gas. *Powder Technol.*, 39: 223-239. DOI: 10.1016/0032-5910(84)85040-8